

REPORT DOCUMENTATION PAGE

Form Approved
OMB No. 0704-0188

Public reporting burden for this collection of information is estimated to average 1 hour per response, including the time for reviewing instructions, searching existing data sources, gathering and maintaining the data needed, and completing and reviewing this collection of information. Send comments regarding this burden estimate or any other aspect of this collection of information, including suggestions for reducing this burden to Department of Defense, Washington Headquarters Services, Directorate for Information Operations and Reports (0704-0188), 1215 Jefferson Davis Highway, Suite 1204, Arlington, VA 22202-4302. Respondents should be aware that notwithstanding any other provision of law, no person shall be subject to any penalty for failing to comply with a collection of information if it does not display a currently valid OMB control number. PLEASE DO NOT RETURN YOUR FORM TO THE ABOVE ADDRESS.

1. REPORT DATE (DD-MM-YYYY)

2. REPORT TYPE

Technical Paper

3. DATES COVERED (From - To)

4. TITLE AND SUBTITLE

5a. CONTRACT NUMBER

5b. GRANT NUMBER

5c. PROGRAM ELEMENT NUMBER
62500F

6. AUTHOR(S)

5d. PROJECT NUMBER
2308

5e. TASK NUMBER
M4S7

5f. WORK UNIT NUMBER
345382

7. PERFORMING ORGANIZATION NAME(S) AND ADDRESS(ES)

8. PERFORMING ORGANIZATION
REPORT

9. SPONSORING / MONITORING AGENCY NAME(S) AND ADDRESS(ES)

Air Force Research Laboratory (AFMC)
AFRL/PRS
5 Pollux Drive.
Edwards AFB CA 93524-7048

10. SPONSOR/MONITOR'S
ACRONYM(S)
XC

11. SPONSOR/MONITOR'S
NUMBER(S)

12. DISTRIBUTION / AVAILABILITY STATEMENT

Approved for public release; distribution unlimited.

13. SUPPLEMENTARY NOTES

See attached 8 papers, all with the information on this page.

14. ABSTRACT

15. SUBJECT TERMS

16. SECURITY CLASSIFICATION OF:

17. LIMITATION
OF ABSTRACT

18. NUMBER
OF PAGES

19a. NAME OF RESPONSIBLE
PERSON

a. REPORT

b. ABSTRACT

c. THIS PAGE

Unclassified

Unclassified

Unclassified

A

Kenette Gfeller

19b. TELEPHONE NUMBER
(include area code)
(661) 275-5016

Standard Form 298 (Rev. 8-98)
Prescribed by ANSI Std. Z39.18

A 90 GHz Phase-Bridge Interferometer for Plasma Density Measurements In the Near Field of a Hall Thruster

Mark Cappelli¹, Wes Hermann, Michael Kodiak, Nicolas Gascon²
Mechanical Engineering Department, Stanford University, Stanford, California
and

William Hargus, Jr.³
Electric Propulsion Laboratory, Air Force Research Laboratories, Edwards AFB, California

Abstract

Preliminary measurements are described of electron number density obtained in the near field of a 200W Busek Hall thruster. The approach taken is ultra-high high frequency (3.3 mm wavelength, 90 GHz) microwave interferometry that affords high spatial resolution suitable for studying the near exit region, where the plasma density can be as high as 10^{11}cm^{-3} . A 90 GHz beam can be focused down to a waist of approximately 7 mm, and over a 50 mm plasma path length, a 10^{11}cm^{-3} plasma density gives rise to an easily measurable 3° phase shift. The system is of a phase-bridge design, utilizing two signal arms split from a fixed frequency source (one passing through the plasma) that recombine at two balanced mixers. A line-integrated electron density is obtained by comparing the two signals from the mixers. This interferometer is suitable for measuring time-dependent plasma density fluctuations offering unprecedented information about plasma turbulence in the near exit region, and the opportunity to study turbulence-enhanced electron transport in regions where the plasma is presumably collisionless and free of interactions with the channel wall.

I. Introduction

One of the most important properties to characterize in a Hall thruster discharge is the near-field plasma (electron or ion) density.[†] Together with the ion velocity, the plasma density provides an independent measurement of the near-field ion current. The local plasma density also serves as a benchmark for thruster simulations, as its established value is sensitive to both the ionization process, and the accelerating electric field. The most commonly used methods of determining the ion density in the near-field of Hall thruster discharges is through the use of either cylindrical Langmuir

probes in current saturation mode [1,2], or guarded ion probes [3], both of which suffer from being intrusive, and from uncertainties in their interpretation due to ion-enhanced secondary electron emission. A measurement of time-average plasma density using probes in the near-field of Hall thrusters is at best accurate to an order of magnitude, and time-resolved measurements must account for limited spectral response of the probe construction. On the other hand, the ease of interpretation and non-intrusive nature of alternative diagnostics such as microwave interferometry makes it an attractive choice for collecting electron (plasma) density data. Microwave interferometry at centimeter-scale wavelengths (e.g., 20 GHz) has been used to study the distant plume region of a Hall thruster. However, its use in studying the near-field is hampered by the limited spatial resolution that can be obtained because the beam waist when focused is at best a few wavelengths in diameter.

In this paper, we present preliminary results of measurements of path-integrated plasma line density in the near-field of a BHT-200 Hall

[†] Hall thrusters are quasi-neutral devices, so the electron and ion densities are to a great extent equal.

¹ Associate Professor, Member AIAA

² Member, AIAA

³ Senior Member, AIAA

Copyright © by Stanford University. Published by
the American Institute of Aeronautics and
Astronautics, Inc., with permission.

20050907 048

thruster [4]. A custom-designed phase-bridge interferometer operating with a 3-mm wavelength solid-state microwave source resulted in modest spatial resolution (~ 7 mm) and lateral and axial surveys of the plasma line-density within 50 mm of the exit plane of the thruster. We also provide a brief discussion of some of the challenges encountered with drifts in the relative sensitivity and phase shift introduced by the mixers, due to heat loading of the microwave components as the entire interferometer is operated in vacuum. These drifts precluded the measurement of plasma density to no better than a factor of about two to four, and were the main source of experimental uncertainty. Because of the interferometer design, measurements can be obtained of the time-variation in the plasma density, and a first direct comparison is made in the non-intrusive plasma density fluctuations, to fluctuations in overall discharge current.

II. Background Theory and Analysis

For collisionless plasmas, the line-integrated electron density can be expressed in terms of the measured phase difference between two identical microwave sources, one of which is passed through the plasma of interest (signal arm), the other serving as a phase reference (reference arm).

The phase difference between these two waves, introduced by the complex impedance of the free electrons, is related to the line-averaged electron density as [5]:

$$\bar{n}_e = \frac{4\pi m_e \epsilon_0 c^2}{e^2 \lambda_0 \ell} \Delta\phi \quad (1)$$

Here m_e is the electron mass, e is the electron charge, c is the speed of light, λ_0 is the free space microwave wavelength, ϵ_0 is the free-space permittivity and ℓ is the plasma column width. Although an interferometry measurement of this sort is averaged along the path of microwave propagation through the plasma, Hall thrusters are reasonably axisymmetric, so that radial variations in the plasma density can be reconstructed from a series of measurements made along paths passing through various

chords of the plume, using standard inverse transform methods (e.g., Abel transformations) or numerical "onion peel" techniques such as those commonly used in optical absorption spectroscopy for characterizing symmetric atomic sources. In a ground test facility, the Hall Thruster can be translated in the axial and radial dimensions, allowing the microwave beam to pass through many sections of the plasma column facilitating this inversion process. The inversion process, which begins from the outermost region of the plasma towards the center, is most accurate where lateral variations in the phase-shift are the greatest. In this paper, no attempt has yet been made to carry out this inversion process.

A schematic (block) diagram of the phase bridge-interferometer configuration used in this study is shown in Fig. 1 below. In the experimental set-up, the output from a 90 GHz fixed frequency Gunn diode with integral oscillator (Millitek model GDM-10-00171R) having a 50mW maximum output power is split into two arms of equal strength through the use of a high directional coupler (Millitek model CSS-10-R090BZ). One arm leads to two variable phase shifters (Millitek models VPS-10-R000N providing a combined 360° phase shift) and level set attenuator (Millitek model LSA-10-R000N). The phase shifters and attenuator serve as a means of calibrating the interferometer. The beam is then launched into the plasma through a standard pyramidal gain horn (Millitek Model SGH-10-RP000) and custom designed matched Teflon lens (50 cm focal length) with an estimated beam waist of ~ 7 mm diameter. The beam is subsequently collected with a second matched lens/horn combination. Both the return arm from the collection horn, and the second arm originating at the diode, are split further into two equal sources with two more highly directional couplers (Millitek model CSS-10-R090BO). The two pairs of source (incident) and return arms are combined in two independently balanced and biased mixers (Millitek model MXB-10-RR0WX). The mixers serve as wave multipliers, with low-pass filters, having a DC-510 MHz IF frequency response. All components of the microwave circuit are

coupled through the use of sections of non-standard length WR-10 waveguides.

For an incident wave $S_i(t) = A_1 \cos(\omega t)$ and return wave $S_r(t) = A_2 \cos(\omega t + \phi)$, the mixer output gives a DC signal proportional to the phase shift $\Delta\phi$ introduced by the plasma:

$$I = \frac{A_1 A_2}{2} \cos \phi \quad (2)$$

The source from one arm is passed through a 90° phase shifter. For the branch that includes 90° phase shifter, the mixer signal is:

$$Q = \frac{A_1 A_2}{2} \cos\left(\frac{\pi}{2} - \phi\right) = \frac{A_1 A_2}{2} \sin(\phi) \quad (3)$$

We see then, that the ratio of the two signals generated in the balanced mixers, $R = I/Q = \tan(\Delta\phi)$. For small phase shifts, where $\tan(\Delta\phi) \approx \Delta\phi$, then this ratio is ideally equal to the phase shift, since the signal amplitudes cancel. In principal, fluctuations in the output of any single mixer signal is proportional to the fluctuations in the plasma density. The ratio of the mixer outputs directly reflects fluctuations in the plasma density.

In practice, the combined branches that give rise to the I and Q signals have unequal intrinsic losses (for example, due to differing waveguide properties and lengths, amongst others). Furthermore, the two mixers themselves may have a different sensitivity to signals at their inputs (α_I , α_Q) and an intrinsic DC offset (I_o , Q_o). As a result, the mixer signals can be represented as:

$$I = I_o + \alpha_I \frac{A_1 A_2}{2} \cos \Delta\phi \quad (3a)$$

$$Q = Q_o + \alpha_Q \frac{A_1 A_2}{2} \sin \Delta\phi \quad (3b)$$

The signals I and Q trace an ellipse in Cartesian space (so-called Smith circles), the center of which is located at position (I_o , Q_o), as illustrated in Fig. 2. In general, a non-zero reference (no plasma) phase shift ϕ_o can arise due to intrinsic phase shifts between the two paths. In Figure 2,

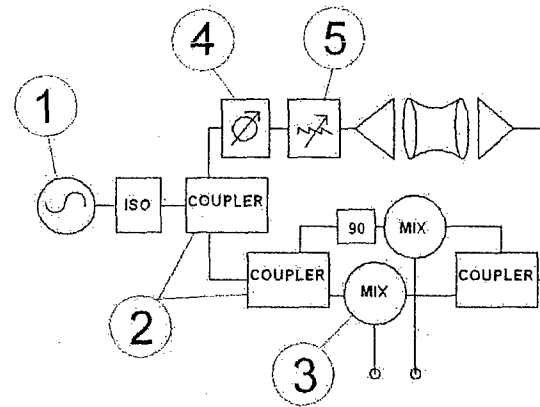


Figure 1. Schematic diagram of the phase bridge-interferometer. 1-90 GHz Gunn Diode, 2-Splitters, 3- Balanced Mixers, 4 - Variable Attenuator, and 5 - Variable Phase Shifter.

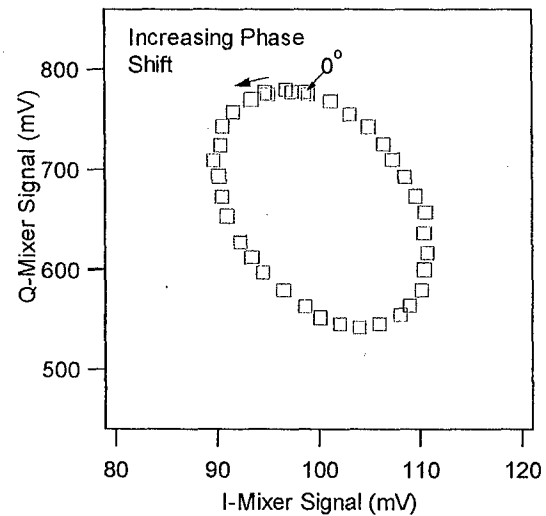


Figure 2. Smith diagram of the microwave interferometer response, obtained by varying the phase setting in the Phase Shifters.

the calibration (Smith) circle is shown for successive 5-degree settings in the variable phase shifter. In this figure, the calibration circles have not been re-scaled for phase shift and DC-offsets. It is noteworthy that the plot is not circular, indicative of the difference in the sensitivity of the two mixers. Figure 3 provides a series of Smith circles obtained while varying the attenuators by 5 dB intervals. In this figure, the calibration circles have been re-scaled for DC offsets and intrinsic phase shift (to the 0 dB circle). Note that although $\ll \sim 1$ dB of

attenuation is expected for the collisionless plume of this discharge, these calibration circles indicate that the variable attenuator introduces an added phase shift which would have to be corrected for when probing collisional plasmas. All analysis presented here use zero-attenuation calibration circles for data reduction.

It is noteworthy that with the interferometer located within the vacuum chamber, and the intrinsic heat dissipation from the powered mixers and diodes (as well as some heat loading from the plume/thruster), noticeable drifts were seen in the sensitivity, phase, and offsets in the mixers. These drifts precluded the measurements of plasma density to no better than a factor of two-five. Since making the measurements discussed here, we have made provisions for active cooling of the components, and improved accuracy and sensitivity is expected from future measurements.

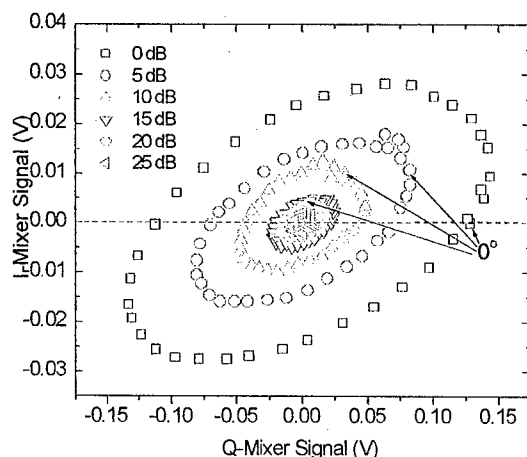


Figure 3. Smith diagram of the microwave interferometer response, obtained by varying the phase setting in the Phase Shifters and attenuation settings in the Variable Attenuator.

Because of possible drifts in the zero-phase reference, our analysis could not rely on the identification of the precise location of the I and Q signals on the calibrated Smith circles when the microwave beam passes through the plasma plume. Instead, an alternate approach to data interpretation is taken here. The analysis of the data for the results presented here is relatively straightforward, and relies on identifying (experimentally), a zero-phase shift reference

point by recording mixer signals (I_{op} , Q_{op}) with the microwave beam passing through regions of the plume where there is little/no plasma. For the small phase shifts anticipated when passing through the near-field plume ($< 5^\circ$), the arc swept along the Smith circle from this zero-phase shift condition, $S = [(I - I_{op})^2 + (Q - Q_{op})^2]^{1/2} = M\Delta\phi$. Here, M is the modulus in the mixer signal at zero-phase, corrected for the DC offset: $M = ((I_{op} - I_o)^2 + (Q_{op} - Q_o)^2)^{1/2}$. The phase shift (and hence plasma density from Equation 1) is determined then, from:

$$\Delta\phi = \frac{S}{M} = \frac{[(I - I_{op})^2 + (Q - Q_{op})^2]^{1/2}}{[(I_{op} - I_o)^2 + (Q_{op} - Q_o)^2]^{1/2}} \quad (4)$$

A representative scan of the $I - I_{op}$ and $Q - Q_{op}$ signals obtained as the thruster is traversed across the microwave beam at an axial position of $z = 95$ mm ($z = 0$ mm is the location of the exit plane) is shown in Fig. 4.

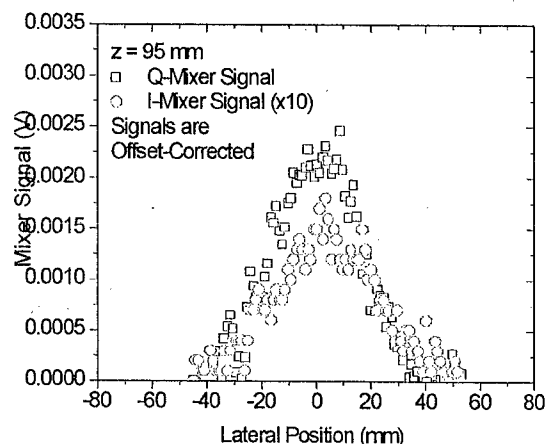


Figure 4. Mixer signals obtained as thruster is traversed across microwave beam.

The Resulting lateral variation in signal S is shown in Fig. 5. An estimate of the modulus, M , for the mixer signal at zero phase in the absence of the plasma, obtained from a calibration circle carried out prior to the measurements, is $M \approx 60$ mV. The measurement of S along with M is used to determine the phase shift, which would have a

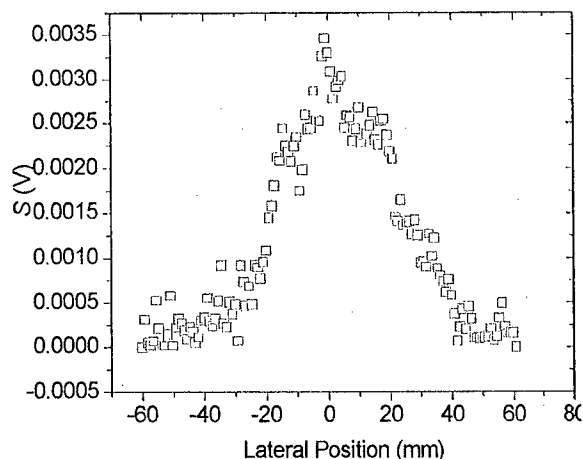


Figure 5. Signal, S corresponding to the arc swept along the Smith circle as the plume traverses the microwave beam.

lateral distribution similar in shape to the signal depicted in Fig. 5.

III. Experiment

A photograph of the interferometer positioned within the vacuum is shown in Fig. 6. To aid in the visualization of the interferometer configuration, a three-dimensional illustration of the interferometer assembly as constructed on a rigid-frame structure is shown in Fig. 7.

The Hall thruster studied here belongs to a family of Busek BHT-200 thrusters, which normally run at a power of approximately 200W. It has an inner wall diameter of 14 mm, and an outer wall diameter of 31 mm (8 mm channel width). The central pole piece extended approximately 7 mm beyond the exit plane of the channel. The channel exit served as the origin position marker for the axial (z) position referred to in the measurements. The cathode was located approximately 20 mm downstream of the central pole piece.

Measurements were carried out in a chamber 1.8 m in diameter and 3 m long with a measured pinging speed of $\sim 32,000$ l/s on xenon, provided by four single-stage cryo panels and one 50 cm diameter two-stage cryo pump. The thruster was operated at nominal conditions of 0.8 A of discharge current, 250V discharge voltage (controlled mode), an anode mass flow

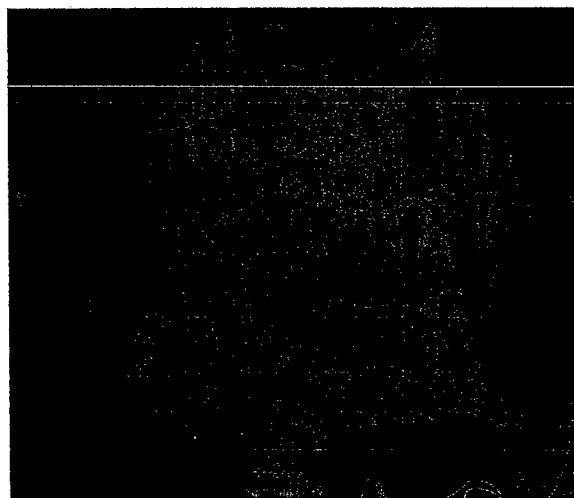


Figure 6. Photograph of interferometer installed in the vacuum chamber.

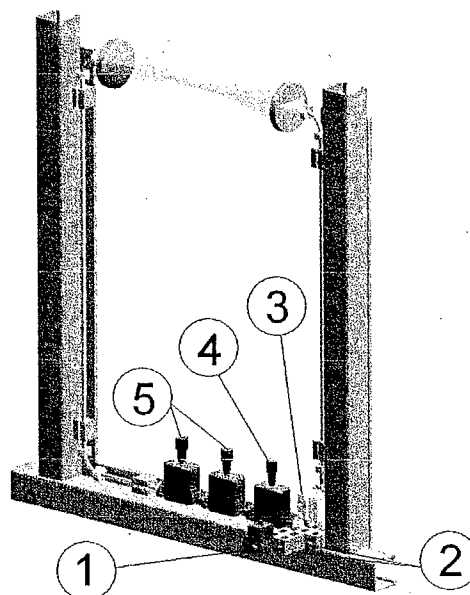


Figure 7. Schematic of the phase - bridge interferometer. 1-90 GHz Gunn Diode, 2- Splitters, 3- Balanced Mixers, 4 - Variable Attenuator, and 5 - Variable Phase Shifter.

rate of 8.5 sccm, and a cathode mass flow rate of 1 sccm.

IV. Results

Measurements were made at nominal discharge operating conditions while translating the Hall thruster through a range of axial (z) and

lateral positions so that the focused microwave beam passes across a chord of the symmetric plume, in a plane normal to the z -direction. Mixer signals were recorded digitally, and the signal modulus S and reference modulus M was then used to determine the phase shift and plasma line-density, $\bar{n}_e \ell$. The variation in this line-density with lateral position is shown in Fig. 8.

The results shown in Fig. 8 have not yet been deconvolved through a radial inversion process even though the deconvolution (Abel inversion) process is greatly simplified if we can assume that the plume is symmetric about the Hall thruster axis. If we were to use the typical width of the distribution shown as a path length (~ 50 mm), then the average plasma density across this 50 mm path length is about $1.6 \times 10^{11} \text{ cm}^{-3}$, consistent with what is expected in the very near field (within one engine diameter) of this Hall thruster, and with the probe measurements of Beale, et al [6]. We have found that in the very near field (e.g., 45 mm), interferences with the microwave beam are introduced by the placement of the cathode (positive lateral positions in the figure), and so data was obtained only for one side of the thruster. It is noteworthy that at larger axial positions, there is an apparent

asymmetry which we attribute to the cathode jet.

Measurements were also taken at a fixed lateral position corresponding to chords passing through the axis of the thruster and varying axial positions. The variation in the plasma line-density with axial position is shown in Fig. 9. The line density is seen to fall exponentially with axial position from the exit plane of the thruster, as expected for a diverging plume. The divergence of the plume is a consequence of the local electrostatic fields, shaped mainly by the applied magnetic field.

This phase-bridge interferometer also provides a non-intrusive means of characterizing temporal fluctuations in the plasma density. For small phase shifts, the output from a single mixer will have a temporal component that is proportional to the fluctuations in the plasma line-density. In the vicinity of the exit plane, large-scale fluctuations are attributed to the so-called "breathing" mode of Hall discharges [7], which arises as a result of the competition between rapid depletion of mass within the channel due to ion acceleration, and the replenishing of xenon through anode injection. This large scale fluctuation is usually identified through analysis of the temporal fluctuation in the discharge current. However, such a "global" parameter may not necessarily reflect the

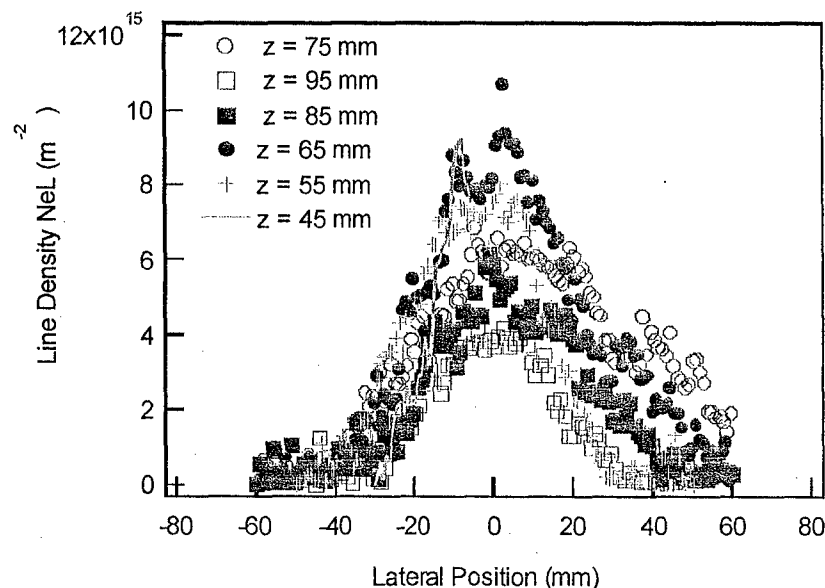


Figure 8. Typical results of plasma line density versus axial position obtained from the interferometer. The exit plane is at $z = 0$ mm. These data have not yet been inverted.

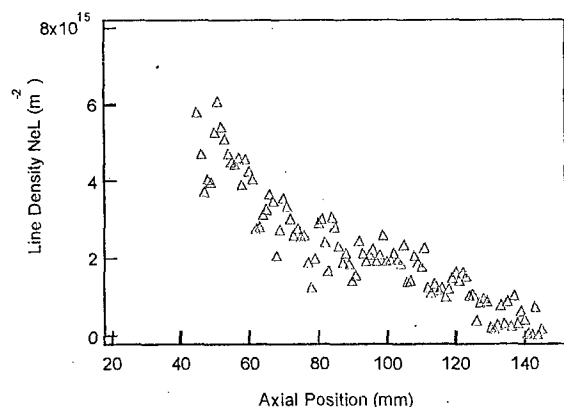


Figure 9. Axial variation in the plasma line-density in the Hall discharge plume.

behavior of the discharge at a particular position, such as the exit plane or near-field of the thruster.

Figure 10 below compares the Fourier spectrum of the current fluctuations to the fluctuation in plasma density seen along a central chord at an axial position of $z = 45$ mm from the exit plane. Apparent in both traces is the relatively strong principal oscillation at about 17 kHz, along with four harmonics. There is a remarkable similarity between the two traces depicted in the figure, which implies that the low-frequency large scale oscillations in the plume plasma density (near-field) is indeed representative of the breathing mode that is ubiquitous in the low frequency oscillations in discharge current.

The microwave diagnostic permits the non-intrusive recording of high frequency ($\gg 100$ kHz) disturbances in the near field of the thruster, which, prior to this, have been characterized nearly exclusively by intrusive probes. The only drawback associated with the application of microwave interferometry to study these fluctuations is that it is a line-of-sight diagnostic, and will resolve only those disturbances that are of relatively large scale – possibly azimuthal waves limited to mode numbers less than $m \approx 3$. A study of these high frequency oscillations will be reported in future papers.

V. Summary

Preliminary measurements are described of electron number density obtained in the near field of a 200W Busek Hall. The approach taken is ultra-high high frequency (3.3 mm wavelength, 90 GHz) microwave interferometry that affords high spatial resolution suitable for studying the near exit region, where the plasma density can exceed 10^{11} cm^{-3} . A 90 GHz beam can be focused down to a waist of approximately 7 mm, and over a 50 mm plasma path length, a 10^{11} cm^{-3} plasma density gives rise to an easily measurable 3° phase shift. The system is of a phase-bridge design, utilizing two signal arms split from a fixed frequency source (one passing through the plasma) that recombine at two balanced mixers. A line-integrated electron density is obtained by comparing the two signals from the mixers. This interferometer is shown to be suitable for measuring time-dependent plasma density fluctuations offering unprecedented information about plasma fluctuations in the near exit region, and the opportunity to study turbulence-enhanced electron transport in regions where the plasma is presumably collisionless and free of interactions with the channel wall.

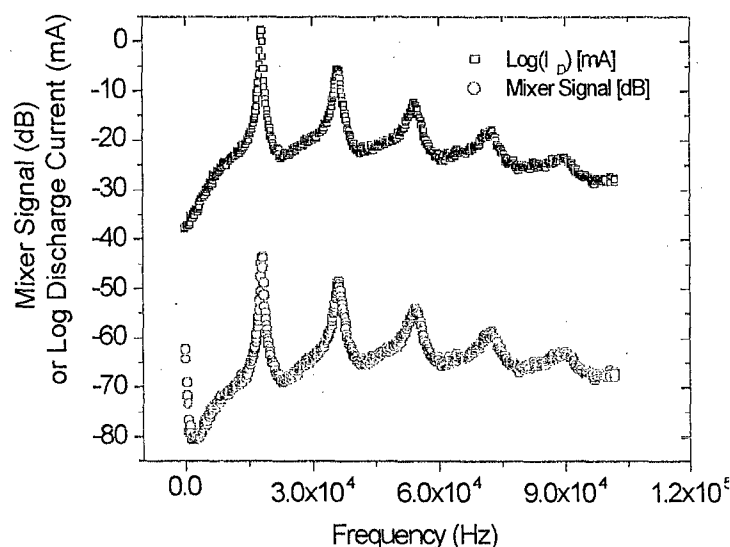


Figure 10. Fourier decomposition of the discharge current (top) and microwave mixer signal (bottom) with the microwave beam passing through the near field ($z = 45$ mm).

Acknowledgements

This research was supported by the Air Force Research Laboratory and the Air Force Office of Scientific Research. Partial support for M.C. was provided through a Summer Fellowship from the National Academy of Science. M.K. and W.H. were supported by the Mechanical Engineering Summer Undergraduate Research Institute at Stanford University.

References

1. A.M. Bishaev and V. Kim, "Local plasma properties in a Hall current accelerator with an extended acceleration zone," *Sov. Phys. Tech. Phys.* **23**, 1055, 1978.
2. G.S. Janes and R.S. Lowder, "Anomalous electron diffusion and ion acceleration in a low-density plasma," *Phys. Fluids* **9**, 1115, 1966.
3. N.B. Meezan and M.A. Cappelli, "Anomalous electron mobility in a coaxial Hall discharge," *Phys. Rev. E* **63**, 026410-1, 2001.
4. W.A. Hargus, Jr. and G. Reed, "The Air Force Clustered Hall Thruster Program," AIAA-2002-3678, 38th Joint Propulsion Conference, July 7-10, Indianapolis, IN, 2002.
5. M. Mitchner and C.H. Kruger, Jr., in *Partially Ionized Gases* (John Wiley and Sons, New York), 1973, p. 161.
6. B. Beal, unpublished measurements of the near field plasma density in a BHT-200, submitted to *AIAA Journal of Propulsion and Power*.
7. E.Y. Choueiri, "Plasma oscillations in Hall thrusters," *Phys. Plasmas*, **8**, 2001.